

An Image Enhancing Pattern-based Sparsity for Real-time Inference on Mobile Devices

Xiaolong Ma^{†1}, Wei Niu^{†2}, Tianyun Zhang³, Sijia Liu⁴, Sheng Lin¹, Hongjia Li¹,
Xiang Chen⁵, Jian Tang⁶, Kaisheng Ma⁷, Bin Ren², Yanzhi Wang¹

¹Northeastern University, ²College of William and Mary, ³Syracuse University,
⁴IBM Watson Lab, ⁵George Mason University, ⁶DiDi AI Labs, ⁷Tsinghua University

ma.xiaol@husky.neu.edu, yanz.wang@northeastern.edu

Abstract

Weight pruning has been widely acknowledged as a straightforward and effective method to eliminate redundancy in Deep Neural Networks (DNN), thereby achieving acceleration on various platforms. However, most of the pruning techniques are essentially trade-offs between model accuracy and regularity which lead to impaired inference accuracy and limited on-device acceleration performance. To solve the problem, we introduce a new sparsity dimension, namely pattern-based sparsity that comprises pattern and connectivity sparsity, and becoming both highly accurate and hardware friendly. With carefully designed patterns, the proposed pruning unprecedentedly and consistently achieves accuracy enhancement and better feature extraction ability on different DNN structures and datasets, and our pattern-aware pruning framework also achieves pattern library extraction, pattern selection, pattern and connectivity pruning and weight training simultaneously. Our approach on the new pattern-based sparsity naturally fits into compiler optimization for highly efficient DNN execution on mobile platforms. To the best of our knowledge, it is the first time that mobile devices achieve real-time inference for the large-scale DNN models thanks to the unique spatial property of pattern-based sparsity and the help of the code generation capability of compilers.

1. Introduction

Deep neural network (DNN) model size has drastically increased due to the amount of available data that is vastly increasing and applications are becoming tremendously sophisticated. To bridge the gap between the performance (inference) requirements of deep learning tasks and the resources availability on the target computing platforms, at the algorithm-level, weight pruning has been proven

[†]These authors contributed equally.

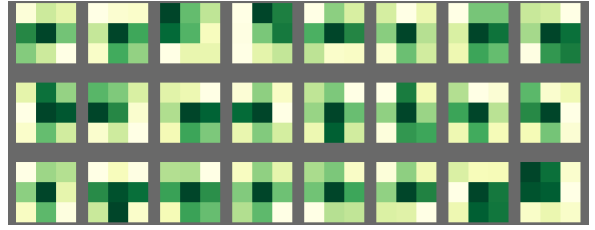


Figure 1. Heat map of randomly selected convolution kernels in the third convolutional layer of a VGG-16 on ImageNet dataset. The weight values in each kernel are normalized and darker shade represents higher absolute value.

to be effective in eliminating redundancy in the original model [11, 9, 7, 23, 34, 15]. There are mainly two types of weight pruning, the non-structured weight pruning and the structured weight pruning, which represent two extremes of the design space. Non-structured pruning [11] achieves high accuracy, but is limited by its hardware unfriendliness [34, 15]. Meanwhile, structured pruning [34] is hardware friendly but suffers from accuracy loss.

It is imperative to seek an approach that can offer, or even go beyond, the best of both types of sparsity. Intuitively, the solution is to design an intermediate sparsity dimension that leverages the advantages of both sparsities above. After visualizing part of the normalized heat map of a pre-trained model of VGG-16 on ImageNet in Figure 1, we find that (i) the effective area (i.e. weights with higher absolute values) forms some specific shapes and repeatedly appears in the model, and (ii) some of the entire convolution kernels have very small weight values and make themselves void kernels. Motivated by the two observations, we introduce a new sparsity dimension – *pattern-based sparsity*, which exploits both intra-convolution and inter-convolution kernel sparsities, exhibiting both high accuracy and regularity, and revealing a previously *unknown* point in design space.

In pattern-based sparsity, we call our intra-convolution kernel sparsity *pattern sparsity* and inter-convolution ker-

nel sparsity *connectivity sparsity*. To get pattern sparsity, we prune a fixed number of weights in each convolution kernel, and the remaining weights form specific “kernel patterns”. Along this line, we find that some carefully designed kernel patterns have special vision properties that potentially enhance image quality, thereby enhancing feature extraction ability of DNNs. For connectivity sparsity, we cut the relatively unimportant connections between certain input and output channels, which is equivalent to removal of corresponding kernels. With connectivity pruning, we enlarge compression rate and reduce the convolution operations of the DNN. To achieve acceleration, our proposed pattern-based sparsity is mobile hardware friendly with help of *code generation* capability of compilers. More specifically, the *filter/kernel re-ordering* technique of compilers can be utilized to maintain instruction-level parallelism and achieve maximum possible hardware acceleration.

At algorithm level, we design a novel pattern-aware network pruning framework that efficiently achieves pattern pruning and connectivity pruning without degrading accuracy. By re-forming the pruning problem into an optimization problem, the framework can solve the pattern and connectivity pruning problems iteratively and analytically by extending the powerful ADMM [4] algorithm. The framework can achieve pattern library generation, pattern assignment, unimportant connectivity removal and weight training simultaneously. Our contributions of this paper are summarized as follows:

- We design a set of patterns, namely pattern library, and prove the image enhancement property that is related to pattern pruning. (Section 4)
- We form a novel pattern-aware network pruning framework that can extract pattern library, perform pattern and connectivity pruning and weight training at the same time. (Section 5)
- We design the corresponding (algorithm-compiler-hardware) inference framework which fully leverages the new sparsity dimension and achieves real-time DNN execution on mobile devices. (Section 6)

Section 7 demonstrates pattern library extraction result, pattern pruning for accuracy and image enhancement results, the overall pattern-based compression results and its acceleration results on mobile devices.

2. Background

DNN model pruning techniques are studied in early work of *non-structured pruning* [10], in which an iterative, heuristic method is used with limited, non-uniform model compression rates. The irregular weight distribution causes irregular memory access and thereby execution overheads,

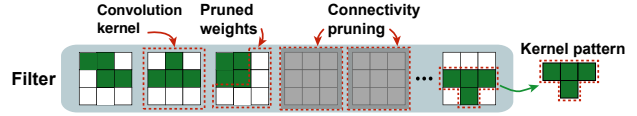


Figure 2. Illustration of pattern-based sparsity.

which leads to limited acceleration performance. *Structured pruning* is pioneered by [34][15], in which regular and smaller weight matrices are generated to eliminate overhead of weight indices and achieve higher acceleration in CPU/GPU executions. However, it suffers from notable accuracy drop when the pruning rate increases. *Kernel level pruning* is studied in [5] that the sparse complimentary kernels can save half of the weights and computations, but it is different from our approach because pattern-based sparsity is theoretically and practically improving the software and hardware performance of DNN while [5] only focuses on parameter and computation reduction without discussing on platform acceleration.

Mobile DNN inference frameworks are studied, including TFLite [1], TVM [6], Alibaba Mobile Neural Network (MNN) [2], DeepCache [35] and DeepSense [36]. These works do not account for model compression techniques, and the performance is far from real-time requirement (usually 30 frames/sec). There are other researches that exploit model sparsity to accelerate DNN inference [19] [27], but they either do not target mobile platforms (require new hardware) or trade off compression rate and accuracy, thus having different challenges than our work.

3. Overview of Pattern-based Sparsity and Compiler-assisted Inference Framework

3.1. Pattern-based Sparsity

The proposed pattern-based sparsity should exploit the best of both non-structured and structured pruning while hiding the disadvantages. Our goal is to achieve high accuracy and execution efficiency simultaneously, through theory and algorithm-level innovation and compiler-level optimizations. Given that, we propose two pattern-based pruning dimensions, *pattern pruning* and *connectivity pruning*.

Pattern pruning is illustrated in Figure 2, where the white blocks denote a fixed number of pruned weights in each kernel. The remaining (four) green blocks in each kernel have arbitrary weight values, while their locations form a specific pattern. Different kernels can have different patterns, but the total number of pattern styles (i.e., the size of the pattern library) shall be limited. We focus on 3×3 kernel pattern in this work because it is widely used in various of DNN architectures. For other kernel shape (e.g., 1×1 or 5×5), we group 1×1 kernels into 3×3 then apply patterns, or use 5×5 patterns directly (will not be discussed in this

work due to space limit).

Connectivity pruning is illustrated in Figure 2, with gray kernels as pruned ones. Connectivity pruning is a good supplement to pattern pruning, as both can be integrated in the same algorithm-level solution and compiler-assisted mobile inference framework.

At theory and algorithm level, we find that the desirable pattern style has connection with Computer Vision concept of the functional steerable filters [8]. At compiler level, the known patterns and connectivity can be reordered and grouped into a regular form, which enables consecutive executions and reduced computations, and maximizing both instruction-level and thread-level parallelism.

3.2. Compiler-assisted Inference Framework

Our compiler-assisted DNN inference framework enables optimized code generation to guarantee end-to-end inference execution efficiency supporting pattern-based sparsity. As the computation paradigm of DNN is in a manner of layerwise execution, we convert a DNN model into computational graph, which is embodied by static C++ (for CPU execution) or OpenCL and CUDA (for GPU execution) codes. The above two pruning schemes can be naturally combined, which achieves high pruning (acceleration) rate while maintaining hardware friendliness.

4. Pattern Library – Theory and Design

4.1. A Unique Perspective on Weight Pruning

Conventionally, weight pruning is considered as a redundant information removal technique. This will inevitably omit other aspects, such as the computer vision properties of pruning. In this work, we consider weight pruning as incorporating an additional convolution mask P on an original kernel. P has the same size as original kernels and binary-valued elements (0 and 1). From our perspective, pattern pruning is an element-wise multiplication of different P 's and original kernels. The set of different P 's is the *pattern library*.

The multi-layer DNN are formed by cascading functional layers. Applying P on every convolution kernel across layers is intrinsically an interpolation operation of P 's. Different patterns can form functional steerable filters [8] (e.g., Gaussian blur filter, sharpen filter, edge detection filter, etc.) by interpolation, and this process only needs a limited number of patterns (i.e., a small pattern library). A small pattern library has two advantages, (i) at algorithm level, an appropriate number of patterns ensures the flexible search space for achieving a solution with good performance on DNN and (ii) at compiler level, fewer patterns means fewer computation paradigms after kernel reordering and grouping, which reduces thread level divergence.

4.2. Pattern Library Design

Our designed patterns could be transformed to a series of steerable filters [8], which in our case, the Gaussian filter and Laplacian of Gaussian filter by interpolating patterns through DNN layers.

Transform patterns to Gaussian filter: Consider a two-dimensional Gaussian filter \mathcal{G} :

$$\mathcal{G}(x, y, \sigma) = \frac{1}{2\pi\sigma^2} e^{-\frac{x^2+y^2}{2\sigma^2}} \quad (1)$$

x and y are input coordinates, and σ^2 is variance.

Binomial coefficients give a compact approximation of the Gaussian coefficients using only integers. To apply the Gaussian filters with 3×3 filter size, we utilize the following approximation. According to (1) and set $\sigma^2 = \frac{1}{2}$, in the 1-D situation, the approximation of Gaussian filter $[1 \ 2 \ 1]$ is given by the convolution of two box filters $[1 \ 1]$. Then we get the 2-D approximation of Gaussian filter by convolving $[1 \ 2 \ 1]$ and $[1 \ 2 \ 1]^T$, and the result is $\begin{bmatrix} 1 & 2 & 1 \\ 2 & 4 & 2 \\ 1 & 2 & 1 \end{bmatrix}$.

Interpolation in multi-layer DNN is proved to be convergent [32]. We can make further approximation by interpolating patterns into convolutional layers (i.e. uniformly map patterns to each kernel). In continuous probability space, interpolating patterns into convolution function is a specific Probability Density Function (PDF), so the effect of interpolating patterns is accumulating probability expectations of interpolation into n convolutional layers.

$$\begin{aligned} & \underbrace{\begin{bmatrix} 1 & 1 & 0 \\ 1 & 1 & 0 \\ 0 & 0 & 0 \end{bmatrix} \dots \begin{bmatrix} 0 & 1 & 1 \\ 0 & 1 & 1 \\ 0 & 0 & 0 \end{bmatrix} \dots \begin{bmatrix} 0 & 0 & 0 \\ 1 & 1 & 0 \\ 1 & 1 & 0 \end{bmatrix} \dots \begin{bmatrix} 0 & 0 & 0 \\ 0 & 1 & 1 \\ 0 & 1 & 1 \end{bmatrix}}_{n \text{ interpolations}} \\ &= \begin{bmatrix} p & 2p & p \\ 2p & 4p & 2p \\ p & 2p & p \end{bmatrix}^n = \begin{bmatrix} 1 & 2 & 1 \\ 2 & 4 & 2 \\ 1 & 2 & 1 \end{bmatrix}^n \end{aligned} \quad (2)$$

The four pattern masks P shown in colored positions in (2) form the Gaussian filter through interpolation. The coefficient p has no effect after normalization.

Transform patterns to Laplacian of Gaussian filter: The Laplacian operator is a second derivative operator. According to the associative property, smoothing an image with Gaussian filter and then applying Laplacian operator is equivalent to convolve the image with the Laplacian of Gaussian (LoG) filter:

$$\nabla^2 \mathcal{G}(x, y, \sigma) = \left(\frac{x^2 + y^2}{\sigma^4} - \frac{2}{\sigma^2} \right) \mathcal{G}(x, y, \sigma) \quad (3)$$

LoG has elegant mathematical properties, and is valid for a variety of applications including image enhancement, edge detection, and stereo matching.

Taylor series expansion is utilized to determine the approximate values of the LoG filter with 3×3 filter size. First, we consider the 1-D situation. The Taylor series expansions of 1-D Gaussian filter $\mathcal{G}(x)$ are given by:

$$\mathcal{G}(x+\delta) = \mathcal{G}(x) + \delta \mathcal{G}'(x) + \frac{1}{2} \delta^2 \mathcal{G}''(x) + \frac{1}{3!} \delta^3 \mathcal{G}'''(x) + \mathcal{O}(\delta^4) \quad (4)$$

$$\mathcal{G}(x-\delta) = \mathcal{G}(x) - \delta \mathcal{G}'(x) + \frac{1}{2} \delta^2 \mathcal{G}''(x) - \frac{1}{3!} \delta^3 \mathcal{G}'''(x) + \mathcal{O}(\delta^4) \quad (5)$$

By summing (4) and (5), we have

$$[\mathcal{G}(x-\delta) - 2\mathcal{G}(x) + \mathcal{G}(x+\delta)]/\delta^2 = \nabla^2 \mathcal{G}(x) + \mathcal{O}(\delta^2) \quad (6)$$

Applying central difference approximation of LoG $\nabla^2 \mathcal{G}(x)$, we derive the 1-D approximation of LoG filter as $\begin{bmatrix} 1 & -2 & 1 \end{bmatrix}$. Then we procure the 2-D approximation of LoG filter by convolving $\begin{bmatrix} 1 & -2 & 1 \end{bmatrix}$ and $\begin{bmatrix} 1 & -2 & 1 \end{bmatrix}^T$, and get $\begin{bmatrix} -1 & 2 & -1 \\ 2 & -4 & 2 \\ -1 & 2 & -1 \end{bmatrix}$ as the *1st approximation*. According to (6), we have

$$\nabla^2 \mathcal{G}(x, y) = \left(\begin{bmatrix} 1 & -2 & 1 \end{bmatrix} + \begin{bmatrix} 1 \\ -2 \\ 1 \end{bmatrix} \right) * \mathcal{G}(x, y) \quad (7)$$

Based on (7), we derive the *2nd approximation* as $\begin{bmatrix} 0 & 1 & 0 \\ 1 & -4 & 1 \\ 0 & 1 & 0 \end{bmatrix}$.

According to the central limit theorem, the convolution of two Gaussian functions is still a Gaussian function. Hence, we convolve the above two approximations of LoG and then apply normalization, and get the *Enhanced Laplacian of Gaussian* (ELoG) filter as $\begin{bmatrix} 0 & 1 & 0 \\ 1 & 8 & 1 \\ 0 & 1 & 0 \end{bmatrix}$.

Similarly, we make the further approximation by interpolating patterns into convolutional layers.

$$\begin{aligned} & \underbrace{\begin{bmatrix} 0 & 1 & 0 \\ 1 & 1 & 1 \\ 0 & 0 & 0 \end{bmatrix} \dots \begin{bmatrix} 0 & 1 & 0 \\ 1 & 1 & 1 \\ 0 & 1 & 0 \end{bmatrix} \dots \begin{bmatrix} 0 & 0 & 0 \\ 1 & 1 & 1 \\ 0 & 1 & 0 \end{bmatrix} \dots \begin{bmatrix} 0 & 1 & 0 \\ 1 & 1 & 1 \\ 0 & 1 & 0 \end{bmatrix}}_{n \text{ interpolations}} \\ &= \begin{bmatrix} 0 & p & 0 \\ p & 1 & p \\ 0 & p & 0 \end{bmatrix}^n = \begin{bmatrix} 0 & 1 & 0 \\ p & 1 & p \\ 0 & 1 & 0 \end{bmatrix}^n \end{aligned} \quad (8)$$

The four pattern masks P shown in colored positions in (8) form the ELoG filter through interpolation. In order to get the best approximation to ELoG filter, we set $p = 0.75$ and $n = 8$, then the desired filter is equal to interpolating these four patterns for eight times. The coefficient p has no effect after normalization.

5. Pattern-Aware Network Pruning Framework for Pattern Library Extraction

In Section 4, we have determined the (eight) patterns as our pattern library through theoretical derivation. However, there are still a couple of open questions. Are these theoretically derived patterns also the most desirable at algorithm level? How to select the appropriate pattern for each kernel and train corresponding (remaining) weights? To answer these questions, we propose a novel *pattern-aware network pruning* framework, simultaneously achieving pattern library extraction (with predefined number of patterns in library), pattern assignment, and weight training.

In pattern library extraction, we start from a large library comprising all possible candidate patterns. By extending ADMM [4], we make convolution kernels dynamically “select” the best suited patterns within the library and train the

unpruned weights. Then we delete the least selected patterns in the library, thereby updating the library. The previous step is iterated on the updated library, with a single step as shown below.

5.1. Pattern Library Extraction – A Single Step

For an N -layer DNN of interest, let \mathbf{W} denote the collection of weights for all 3×3 kernels, i.e., $\mathbf{W} = \{\mathbf{W}_i\}_{i=1}^N$. The pattern of each kernel \mathbf{W}_i is restricted to a finite pattern library $\Omega = \{\mathbf{M}_1, \dots, \mathbf{M}_j, \dots, \mathbf{M}_K\}$, where \mathbf{M}_j denotes a binary mask, and K denotes the total number of possible patterns. We choose to reserve 4 non-zero entries in a kernel to match the SIMD (single-instruction multiple-data) architecture of embedded CPU/GPU processors, thereby maximizing throughput. As a result, the initial $K = \binom{9}{4} = 126$, and K will decrease in each step.

The purpose of each step is to select a pattern from the current library for each kernel, and train the non-zero weights. Let $f(\mathbf{W}; \mathcal{D})$ denote the training loss (\mathcal{D} denotes training data), we pose the following optimization problem

$$\begin{aligned} & \underset{\mathbf{W}, \mathbf{z}}{\text{minimize}} && f(\{\mathbf{W}_i \circ (\sum_{j=1}^K z_j \mathbf{M}_j)\}_{i=1}^N; \mathcal{D}) \\ & \text{subject to} && z_j \in \{0, 1\}, \forall j, \quad \sum_{j=1}^K z_j = 1, \end{aligned} \quad (9)$$

where z_j denotes the Boolean selection variable to indicate which pattern in Ω is chosen for \mathbf{W}_i . The constraint $\sum_{j=1}^K z_j = 1$ indicates that only one pattern is selected, and thus $\mathbf{W}_i \circ (\sum_{j=1}^K z_j \mathbf{M}_j)$ denotes the pattern-pruned kernel using one of pruning patterns. Here \circ denotes element-wise product. In (9), we have *two* types of optimization variables: (i) 3×3 kernel weights \mathbf{W} , (ii) pattern Boolean selection variables $\mathbf{z} \in [0, 1]^K$. The pattern selection scheme is co-optimized with non-zero weight training.

To solve the above problem analytically, we introduce auxiliary variables \mathbf{u} together with constraints $\mathbf{z} = \mathbf{u}$. Based on that, we reformulate problem (9) as

$$\begin{aligned} & \underset{\mathbf{W}, \mathbf{u}}{\text{minimize}} && f(\{\mathbf{W}_i \circ (\sum_{j=1}^K z_j \mathbf{M}_j)\}_{i=1}^N; \mathcal{D}) + \mathcal{I}(\mathbf{u}) \\ & \text{subject to} && \mathbf{z} = \mathbf{u} \end{aligned} \quad (10)$$

where $\mathcal{I}(\mathbf{u})$ is the indicator function

$$\mathcal{I}(\mathbf{u}) = \begin{cases} 0 & \text{if } u_j \in [0, 1], \forall j, \quad \sum_{j=1}^K u_j = 1 \\ \infty & \text{otherwise.} \end{cases} \quad (11)$$

Here we relax the binary selection variable $z_i \in \{0, 1\}$ to the (continuous) probabilistic selection variable $u_i \in [0, 1]$.

The augmented Lagrangian function of problem (10) is given by

$$\begin{aligned} \mathcal{L}(\mathbf{W}, \mathbf{z}, \mathbf{u}, \boldsymbol{\mu}) &= f(\{\mathbf{W}_i \circ (\sum_{j=1}^K z_j \mathbf{M}_j)\}_{i=1}^N; \mathcal{D}) \\ &+ \mathcal{I}(\mathbf{u}) + \boldsymbol{\mu}^T (\mathbf{z} - \mathbf{u}) + \frac{\rho}{2} \|\mathbf{z} - \mathbf{u}\|_2^2 \end{aligned} \quad (12)$$

where μ is Lagrangian multipliers, and $\|\cdot\|_2$ denotes the Frobenius norm. $\rho > 0$ is a given augmented penalty value, and for ease of notation we view matrices as *vectors* in optimization.

ADMM [4] is then given by the following alternating optimization process. At iteration t , ADMM yields

$$\begin{aligned} \mathbf{W}^{(t)}, \mathbf{z}^{(t)} &= \arg \min_{\mathbf{W}, \mathbf{z}} \mathcal{L}(\mathbf{W}, \mathbf{z}, \mathbf{u}^{(t-1)}, \mu^{(t-1)}) \quad (\text{Primal}) \\ \mathbf{u}^{(t)} &= \arg \min_{\mathbf{u}} \mathcal{L}(\mathbf{W}^{(t)}, \mathbf{z}^{(t)}, \mathbf{u}, \mu^{(t-1)}) \quad (\text{Proximal}) \\ \mu^{(t)} &= \mu^{(t-1)} + \rho(\mathbf{z}^{(t)} - \mathbf{u}^{(t)}), \end{aligned} \quad (13)$$

where the initial values $\mathbf{u}^{(0)}$ and $\mu^{(0)}$ are given.

Problem (Primal) can be simplified to

$$\begin{aligned} \underset{\mathbf{W}, \mathbf{z}}{\text{minimize}} \quad & f(\{\mathbf{W}_i \circ (\sum_{j=1}^K z_j \mathbf{M}_j)\}_{i=1}^N; \mathcal{D}) + \frac{\rho}{2} \|\mathbf{z} - \mathbf{a}\|_2^2 \end{aligned} \quad (14)$$

where $\mathbf{a} := (\mathbf{u}^{(t-1)} - (1/\rho)\mu^{(t-1)})$. In problem (14), the objective function is differentiable, and can thus be solved by standard DNN solvers in SGD.

Problem (Proximal) can be equivalently decomposed over \mathbf{u} . This leads to problem

$$\begin{aligned} \underset{\mathbf{u}}{\text{minimize}} \quad & \frac{\rho}{2} \|\mathbf{u} - \mathbf{d}\|_2^2 \\ \text{subject to} \quad & u_j \in [0, 1], \forall j, \quad \sum_{j=1}^K u_j = 1, \end{aligned} \quad (15)$$

where $\mathbf{d} := \mathbf{z}^{(t)} + (1/\rho)\mu^{(t-1)}$.

Based on [28], the analytical solution to problem (15) is

$$\mathbf{u}^{(t)} = [\mathbf{d} - \nu \mathbf{1}]_+, \quad (16)$$

where $[x]_+ = x$ if $x \geq 0$ and 0 otherwise, ν is the root of the equation

$$\mathbf{1}^T [\mathbf{d} - \nu \mathbf{1}]_+ = 1. \quad (17)$$

Once \mathbf{W} and \mathbf{z} are solved, \mathbf{z} is a continuous variable rather than a binary variable. We need an intermediate step to project continuous \mathbf{z}_{admm} to integer $\mathbf{z}_{\text{binary}}$, yielding

$$\begin{aligned} \underset{\mathbf{z}_{\text{binary}}}{\text{minimize}} \quad & \|\mathbf{z}_{\text{binary}} - \mathbf{z}_{\text{admm}}\|_2^2 \\ \text{subject to} \quad & \mathbf{1}^T \mathbf{z} = 1, z_i \in \{0, 1\}, \forall i. \end{aligned} \quad (18)$$

The solution is given by $[\mathbf{z}_{\text{binary}}]_i = 1$ if $i = \arg \max_j [\mathbf{z}_{\text{admm}}]_j$, and 0 otherwise. At this point, we have simultaneously selected pattern for each kernel and trained the non-zero weights.

5.2. Pattern Library Extraction – Overall

The overall pattern library extraction starts from $K = 126$ and decreases K in each step, with algorithm brief shown in Algorithm 1. In actual implementation we set the

new K to be 12 in the first step as most of the patterns occur in very few times. We set the target K to be either 12, 8, or 4. When the type of patterns is within this range, the overhead in code generation at compiler level can be kept small and parallelism can be maximized.

Total Runtime: Despite an iterative process, the total number of epochs (and training time) can be limited. This is because except for the last step, we only need to extract a number of patterns instead of finishing the final training of non-zero weights. As a result, we can finish each step with 10% to 20% of the total epochs as training of the original DNN. In the last step, we need around 10 ADMM iterations, each requiring less than 20% of the total epochs of original DNN training. So the total number of training epochs using PyTorch [29] is around 300 - 400 for the whole process, which is even lower compared with many prior art [10, 25].

Algorithm 1: Pattern library extraction process.

```

1 Initialization:  $\Omega = \{\mathbf{M}_1, \mathbf{M}_2, \dots, \mathbf{M}_K\}$  with  $K = 126$ ;
   Result: Subsets  $\Omega'$  with  $K = 12, 8$  or  $4$ ;
2 while training neural network do
3   Update  $W$  by solving (Primal);
4   for  $K \leftarrow 126$  until  $K = 12, 8$  or  $4$  do
5     Solving (Proximal) using current  $\Omega$ ;
6     Update  $\mu$  in (13);
7     Calculate pattern distribution of current  $\Omega$ ;
8     Removing patterns with fewest occurrences in  $\Omega$ ;
9   end
10 end

```

6. Connectivity Sparsity and the New Sparsity Induced Inference Framework

From Section 5, we have designed the algorithm level solution to simultaneously achieve pattern library extraction, pattern selection and weight training. In this section, we discuss the connectivity sparsity and how to use the same solution framework to achieve the combination of pattern sparsity and connectivity sparsity. We also design a compiler-assisted DNN inference framework for mobile platforms, which can fully leverages the regularity in this new sparsity type, and potentially surpasses the hardware performances with many prior works.

6.1. Connectivity Sparsity

Connectivity sparsity is achieved by connectivity pruning which can be integrated in the same algorithm-level solution in Section 5.1 and compiler-assisted mobile inference framework. Using the same notations as in Section 5.1, we define the collection of weights in i -th layer as $\mathbf{W}_i \in \mathbb{R}^{H_i \times W_i \times F_i \times C_i}$, where H and W denote the dimension of the convolution kernel. F and C denote the number of filters and channels, respectively. We further define criti-

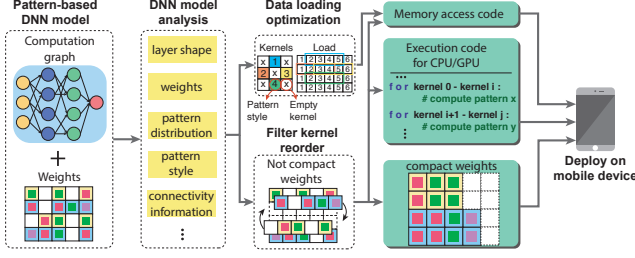


Figure 3. Overview of the compiler level DNN inference framework for mobile devices.

cal connectivity score for each convolution kernel as

$$\gamma = ||[\mathbf{W}_i]_{:,f,c}||_2 \quad (19)$$

where f and c are filter and channel indices, respectively. The problem formulation and solution framework for achieving connectivity sparsity is similar with the ones in Section 5.1. The difference is that the constraint in the framework is related to γ . Please note that our algorithm level solution can solve the problems of pattern pruning and connectivity pruning simultaneously or individually. Due to space limit, the connectivity pruning solution details are described in Supplemental Materials.

6.2. Compiler-assisted Inference Framework for Real-time Execution

After we obtain pattern and connectivity sparsity combined in a DNN model, we use a compiler-assisted inference framework that shows in Figure 3 to maximize the execution efficiency by utilizing multiple optimization techniques that are induced by pattern-based sparsity.

Layerwise optimization for DNN computation graph is designed to achieve the best of instruction-level and thread-level parallelism by utilizing the unique filter/kernel re-ordering technique as Figure 3 shows. In the weight matrix illustration, the internal squares with different colors denote different pattern styles, and empty white squares denote connectivity sparsity. By filter/kernel re-ordering, we (i) organize the filters with similar kernels together to improve *inter-thread* parallelism, and (ii) group kernels with identical patterns in each filter together to improve *intra-thread* parallelism. By DNN computation graph optimization, the generated execution code eliminates all of the execution branches, implying higher instruction-level parallelism; meanwhile, similar filter groups escalate execution similarity and result in a good load balance, achieving better thread-level parallelism.

Memory access optimizations for hardware execution address the poor memory performance due to the irregular memory access. In DNN execution, the input/output data access is associated with the non-zero elements of the weights. Since in pattern-based sparse model, the non-zero

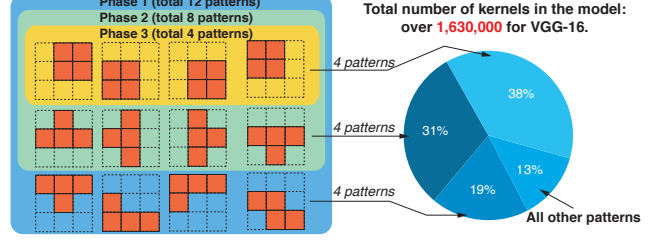


Figure 4. The pattern library extraction result.

pattern of each kernel is already known, we can generate data access code with this information for each kernel pattern and call them dynamically during DNN execution. With the data access code, it is possible to directly access valid input data that is associated with the non-zero elements in a pattern-based kernel. Moreover, after DNN computation graph optimization, the model weights distribution is highly compact and structured as Figure 3 shows, which reduces the calling frequency of data access code and as a result, reduces the memory overhead.

7. Experimental Results

In our experiment, our generated pattern-based sparse models are based on four widely used network structures, VGG-16 [31], ResNet-18/50 [12] and MobileNet-V2 [16], and are trained on an eight NVIDIA RTX-2080Ti GPUs server using PyTorch [29]. We show the consistency of pattern library extraction results with the theoretically designed pattern library in Section 4.2, and provide the accuracy improvement and image enhancement demonstrations. We also show the overall compression results of pattern-based pruning in different DNN models. In order to show acceleration of pattern-based sparsity on mobile devices, we compare it with three state-of-the-art DNN inference acceleration frameworks, TFLite [1], TVM [6], and MNN [2].

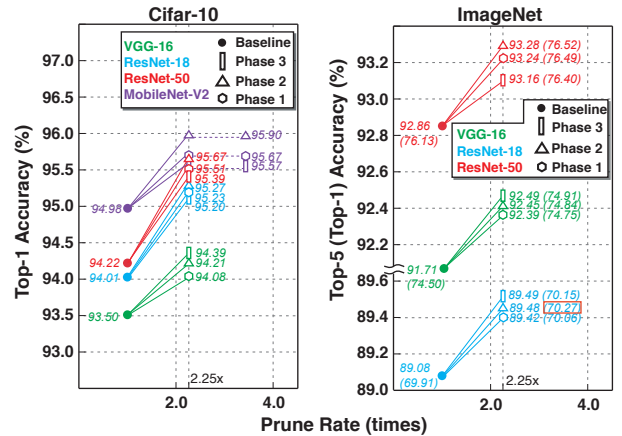


Figure 5. Accuracy improvement results from pattern pruning on different DNN models and datasets (CIFAR-10 & ImageNet).

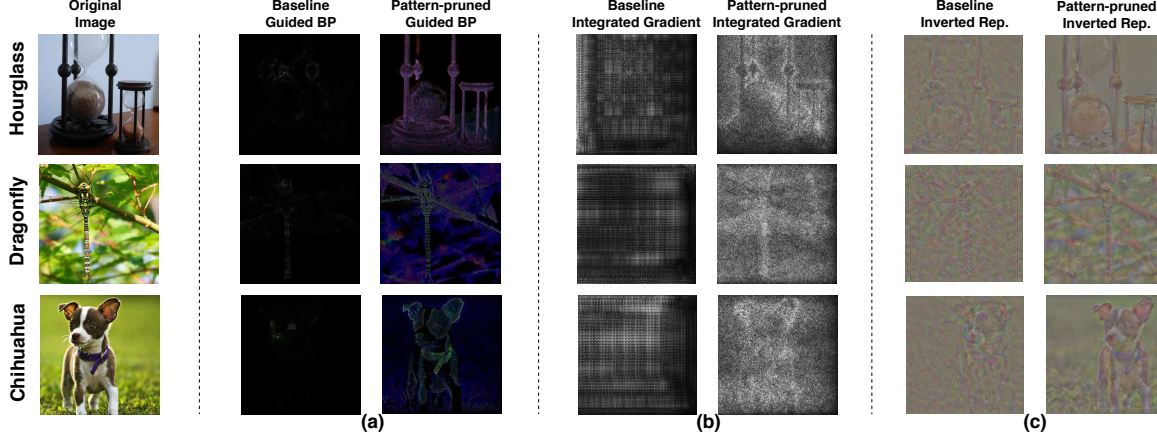


Figure 6. Visualization comparisons of three images from ImageNet dataset on original and pattern pruned VGG-16 model using (a) guided-backpropagation (BP); (b) integrated gradients and (c) inverted representation methods.

Our experiments are conducted on a Samsung Galaxy S10 cell phone with the latest Qualcomm Snapdragon 855 mobile platform that consists of a Qualcomm Kryo 485 Octa-core CPU and a Qualcomm Adreno 640 GPU.

7.1. Pattern Library Extraction Result

We use VGG-16 on ImageNet dataset to extract pattern libraries. VGG-16 has more than 1,630,000 convolution kernels. However, patterns can be concentrated to 12 styles in only a couple of steps. Figure 4 shows the pattern styles distribution results when K decreases to 32 after two steps. We can see that most of the patterns are distributed in the top 12 styles, namely Phase 1 pattern library. If we continue to decrease K to 8, the remaining 8 patterns form Phase 2 pattern library. We can notice that Phase 2 is *exactly the same* with our derived pattern library in Section 4.2. Further extraction step will give us Phase 3 pattern library, which is the top-4 pattern styles. Using other DNNs and datasets gives us the same extraction results, thereby we can conclude that the theoretically derived patterns are also the most desirable ones at algorithm level.

7.2. Accuracy Analysis and Visualization Demonstration for Pattern Pruning

Accuracy evaluation is shown in Figure 5. Starting from the baseline accuracy results that are in many cases higher than prior works, we have the first conclusion that *the accuracy improvements are more significant when applying the designed 8 patterns (i.e., pattern library at Phase 2) on each convolution kernel*. The accuracy improvements are consistently observed on various network structures (e.g., VGG-16, ResNet-18/50, MobileNet-V2) on CIFAR-10 and ImageNet datasets.

Visualization comparisons of applying Phase 2 pattern library to an original DNN model (*pattern pruning*) are demonstrated in Figure 6. To ensure the fairness in com-

parisons, we adopt three visualization methods to eliminate the impact of causal factors. They are (a) *Guided-backpropagation (BP)* [33], (b) *Integrated gradients* [26], and (c) *Inverted representation* [3]. Through different visualization techniques, we can see what a DNN has learned and how well it can preserve the photographically accurate information from an image.

We provide strong evidence in Figure 6 that pattern pruned VGG-16 model can effectively capture more image details and less noise compared with the original VGG-16 model. We conclude that the accuracy improvement is attributed to the enhanced image processing ability of our designed pattern library.

7.3. Connectivity Pruning and Overall Model Compression Results

Combining connectivity sparsity with pattern sparsity has different DNN performances with different pattern libraries. Figure 7 illustrates testing accuracies of training

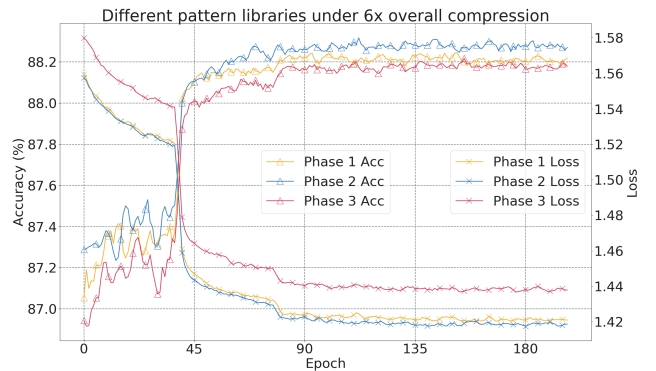


Figure 7. ResNet-18 on ImageNet top-5 test accuracy records in training connectivity sparsity combined with pattern sparsity. We use overall $6\times$ compression to illustrate training performance on different pattern libraries.

Table 1. Pattern-based pruning results on CIFAR-10 using VGG-16 and ResNet-18/50.

	Method	Base Accuracy	Prune Accuracy	CONV Comp. Rate	Sparsity (Pattern) Type
ResNet-18	AMC [14]	90.5%	90.2%	2.0×	Structured
	Variational Pruning [38]	92.0%	91.7%	1.6×	Structured
	Our's	94.0%	94.7%	8.0×	Phase 2
	Our's	94.0%	94.6%	12.0×	Phase 3
	Our's	94.0%	94.2%	16.0×	Phase 2
ResNet-50	One Shot Pruning [21]	93.8%	93.6%	2.5×	Irregular
	AMC [14]	93.5%	93.5%	1.7×	Structured
	Our's	94.2%	95.2%	8.0×	Phase 3
	Our's	94.2%	94.9%	12.0×	Phase 3
	Our's	94.2%	94.5%	16.0×	Phase 3
VGG-16	Iterative Pruning [11, 21]	92.5%	92.2%	2.0×	Irregular
	One Shot Pruning [21]	92.5%	92.4%	2.5×	Irregular
	2PFPCE [24]	92.9%	92.8%	4.0×	Structured
	Efficient ConvNet [18]	93.2%	93.4%	2.7×	Structured
	Our's	93.5%	93.4%	8.0×	Phase 2
	Our's	93.5%	93.3%	11.6×	Phase 2
	Our's	93.5%	93.2%	19.7×	Phase 1

Table 2. Pattern-based pruning results on ImageNet using VGG-16 and ResNet-18/50.

	Method	Base Top-1/5 Accuracy	Prune Top-1/5 Accuracy	CONV Comp. Rate	Sparsity (Pattern) Type
ResNet-18	Network Slimming [20]	68.9/88.7%	67.2/87.4%	1.4×	Structured
	DCP [39]	69.6/88.9%	64.1/85.7%	3.3×	Structured
	Our's	69.9/89.1%	69.5/89.2%	4.0×	Phase 2
	Our's	69.9/89.1%	68.2/88.3%	6.0×	Phase 2
	Our's	69.9/89.1%	67.1/87.7%	8.0×	Phase 2
ResNet-50	Fine-grained [23]	N/A	N/A/92.3%	2.6×	Irregular
	ADMM-NN [30]	N/A	N/A/92.3%	7.0×	Irregular
	AutoSlim [37]	76.1/N/A%	72.2/N/A%	3.1×	Structured
	ThiNet [22]	72.9/91.1%	68.4/88.3%	3.3×	Structured
	Soft Filter Prune [13]	76.1/92.8%	74.6/92.1%	1.7×	Structured
	Our's	76.1/92.9%	75.9/92.7%	3.9×	Phase 2
	Our's	76.1/92.9%	75.8/92.8%	4.9×	Phase 3
VGG-16	Deep compression [10]	68.8/89.1%	68.5/88.7%	3.5×	Irregular
	NeST [7]	71.6/90.4%	69.3/89.4%	6.5×	Irregular
	ADMM-NN [30]	68.8/89.1%	68.7/88.9%	10.2×	Irregular
	APoZ [17]	N/A/88.4%	66.2/87.6%	2.0×	Structured
	Our's	74.5/91.7%	74.4/91.5%	8.0×	Phase 2
	Our's	74.5/91.7%	74.1/91.3%	10.0×	Phase 2
	Our's	74.5/91.7%	73.6/91.0%	12.0×	Phase 2

connectivity sparsity combined with existing pattern sparsity. From diagram, we can clearly notice that by using designed pattern library (Phase 2), we can achieve better training performance, thereby higher DNN accuracy. Similar paradigm can be observed with different compression rates and on different networks/datasets. Due to the space limit, we only show the ResNet-18 on ImageNet training with overall 6× compression rate diagram. More diagrams with different overall compression rates using VGG-16 and ResNet-50 on CIFAR-10 and ImageNet datasets are shown in the Supplemental Materials. Please note that pattern sparsity already reserves 2.25× compression rate, and we add different connectivity compression rates upon it to achieve the different overall compression rates. Table 1 and Table 2 record the best final DNN accuracies and compression rates regarding their pattern styles, and are compared with several pruning methods with their sparsity types.

7.4. Performance Evaluation on Mobile Platform

In this part, we demonstrate our evaluation results on mobile device to show the real-time inference of our proposed pattern-based sparse model with the help of the compiler-assisted inference framework. To guarantee fairness, all frameworks are using the same pattern-based sparse model, and we also enable the fully optimized configurations of TFLite, TVM and MNN (e.g., Winograd optimization is turned on).

Execution time. Figure 8 shows mobile CPU/GPU execution time of pattern-based model on different platforms. Since Phase 2 pattern library has best performance on pruning, our testing model are using Phase 2 patterns and 8× overall compression rate for ResNet-18, 5.8× for ResNet-50 and 12× for VGG-16. The inference is using images from ImageNet dataset. To save space, we put the CIFAR-10 execution time results in the Supplemental Material. We can see our approach achieves significant acceleration on mobile device compared with other frameworks. Real-time execution usually requires 30 frames/sec (i.e., 33ms/frame). From our results, all of our DNN models on ImageNet meet or far exceed this requirement, and some of them can even accomplish real-time inference on mobile CPU.

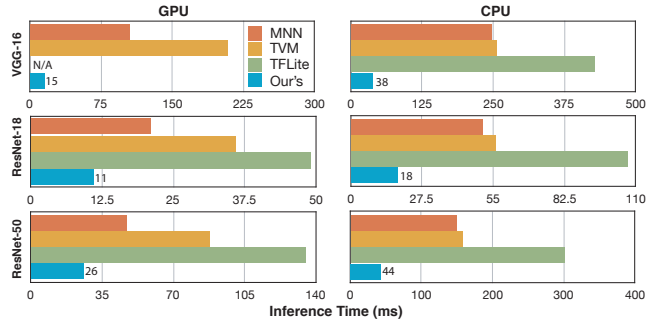


Figure 8. Inference time (ms) comparisons for different mobile inference frameworks using image from ImageNet dataset.

8. Conclusion

This paper proposes pattern-based sparsity, along with the highly efficient algorithm level pruning framework and the novel compiler level inference framework. Pattern-based sparsity inherits the flexibility from non-structured sparsity and regularity from structured sparsity, achieving both highly accurate/compressed model and hardware friendliness. Particularly, with carefully designed pattern library, pattern pruning achieves image enhancement and accuracy improvement. The pattern-based sparsity elicits compiler optimization, achieving real-time inference on mobile devices on various representative large-scale DNNs.

References

- [1] <https://www.tensorflow.org/mobile/tflite/>. 2, 6
- [2] <https://github.com/alibaba/MNN>. 2, 6
- [3] Mahendran Aravindh and Vedaldi Andrea. Understanding deep image representations by inverting them. In *Computer Vision and Pattern Recognition, 2015. CVPR 2015. IEEE Conference on*, 2015. 7
- [4] Stephen Boyd, Neal Parikh, Eric Chu, Borja Peleato, and Jonathan Eckstein. Distributed optimization and statistical learning via the alternating direction method of multipliers. *Foundations and Trends® in Machine Learning*, 3(1):1–122, 2011. 2, 4, 5
- [5] Chun-Fu Chen, Jinwook Oh, Quanfu Fan, and Marco Pistoia. Sc-conv: Sparse-complementary convolution for efficient model utilization on cnns. In *2018 IEEE International Symposium on Multimedia (ISM)*, pages 97–100. IEEE, 2018. 2
- [6] Tianqi Chen, Thierry Moreau, Ziheng Jiang, Lianmin Zheng, Eddie Yan, Haichen Shen, Meghan Cowan, Leyuan Wang, Yuwei Hu, Luis Ceze, et al. TVM: An automated end-to-end optimizing compiler for deep learning. In *OSDI*, 2018. 2, 6
- [7] Xiaoliang Dai, Hongxu Yin, and Niraj K Jha. Nest: a neural network synthesis tool based on a grow-and-prune paradigm. *arXiv preprint arXiv:1711.02017*, 2017. 1, 8
- [8] W.T. Freeman and E.H. Adelson. The design and use of steerable filters. In *IEEE Transactions on Pattern Analysis and Machine Intelligence*, volume 13, pages 891–906. IEEE, 1991. 3
- [9] Yiwen Guo, Anbang Yao, and Yurong Chen. Dynamic network surgery for efficient dnns. In *Advances In Neural Information Processing Systems*, pages 1379–1387, 2016. 1
- [10] Song Han, Huizi Mao, and William J Dally. Deep compression: Compressing deep neural networks with pruning, trained quantization and Huffman coding. *arXiv preprint arXiv:1510.00149*, 2015. 2, 5, 8
- [11] Song Han, Jeff Pool, John Tran, and William Dally. Learning both weights and connections for efficient neural network. In *Advances in Neural Information Processing Systems*, pages 1135–1143, 2015. 1, 8
- [12] Kaiming He, Xiangyu Zhang, Shaoqing Ren, and Jian Sun. Deep residual learning for image recognition. In *Proceedings of the IEEE Conference on Computer Vision and Pattern Recognition*, pages 770–778, 2016. 6
- [13] Yang He, Guoliang Kang, Xuanyi Dong, Yanwei Fu, and Yi Yang. Soft filter pruning for accelerating deep convolutional neural networks. In *International Joint Conference on Artificial Intelligence (IJCAI)*, pages 2234–2240, 2018. 8
- [14] Yihui He, Ji Lin, Zhijian Liu, Hanrui Wang, Li-Jia Li, and Song Han. Amc: Automl for model compression and acceleration on mobile devices. In *European Conference on Computer Vision*, pages 815–832, 2018. 8
- [15] Yihui He, Xiangyu Zhang, and Jian Sun. Channel pruning for accelerating very deep neural networks. In *Computer Vision (ICCV), 2017 IEEE International Conference on*, pages 1398–1406. IEEE, 2017. 1, 2
- [16] Andrew G Howard, Menglong Zhu, Bo Chen, Dmitry Kalenichenko, Weijun Wang, Tobias Weyand, Marco Andreetto, and Hartwig Adam. Mobilenets: Efficient convolutional neural networks for mobile vision applications. *arXiv preprint arXiv:1704.04861*, 2017. 6
- [17] Hengyuan Hu, Rui Peng, Yu-Wing Tai, and Chi-Keung Tang. Network trimming: A data-driven neuron pruning approach towards efficient deep architectures. *arXiv preprint arXiv:1607.03250*, 2016. 8
- [18] Hao Li, Asim Kadav, Igor Durdanovic, Hanan Samet, and Hans Peter Graf. Pruning filters for efficient convnets. *arXiv preprint arXiv:1608.08710*, 2016. 8
- [19] Baoyuan Liu, Min Wang, Hassan Foroosh, Marshall Tappen, and Marianna Pinsky. Sparse convolutional neural networks. In *CVPR*, pages 806–814, 2015. 2
- [20] Zhuang Liu, Jianguo Li, Zhiqiang Shen, Gao Huang, Shoumeng Yan, and Changshui Zhang. Learning efficient convolutional networks through network slimming. In *Proceedings of the IEEE International Conference on Computer Vision*, pages 2736–2744, 2017. 8
- [21] Zhuang Liu, Mingjie Sun, Tinghui Zhou, Gao Huang, and Trevor Darrell. Rethinking the value of network pruning. *arXiv preprint arXiv:1810.05270*, 2018. 8
- [22] Jian-Hao Luo, Jianxin Wu, and Weiyao Lin. Thinet: A filter level pruning method for deep neural network compression. In *Proceedings of the IEEE international conference on computer vision*, pages 5058–5066, 2017. 8
- [23] Huizi Mao, Song Han, Jeff Pool, Wenshuo Li, Xingyu Liu, Yu Wang, and William J Dally. Exploring the regularity of sparse structure in convolutional neural networks. *arXiv preprint arXiv:1705.08922*, 2017. 1, 8
- [24] Chuhan Min, Aosen Wang, Yiran Chen, Wenyao Xu, and Xin Chen. 2pfpc: Two-phase filter pruning based on conditional entropy. *arXiv preprint arXiv:1809.02220*, 2018. 8
- [25] Pavlo Molchanov, Stephen Tyree, Tero Karras, Timo Aila, and Jan Kautz. Pruning convolutional neural networks for resource efficient inference. *arXiv preprint arXiv:1611.06440*, 2016. 5
- [26] Sundararajan Mukund, Taly Ankur, and Yan Qiqi. Axiomatic attribution for deep networks. In *2017 International Conference on Machine Learning (ICML)*. ACM/IEEE, 2017. 7
- [27] Angshuman Parashar, Minsoo Rhu, Anurag Mukkara, Antonio Puglielli, Rangharajan Venkatesan, Brucek Khailany, Joel Emer, Stephen W Keckler, and William J Dally. Scnn: An accelerator for compressed-sparse convolutional neural networks. In *ISCA*, 2017. 2
- [28] Neal Parikh and Stephen Boyd. Proximal algorithms. *Foundations and Trends® in Optimization*, 1(3):127–239, 2014. 5
- [29] Adam Paszke, Sam Gross, Soumith Chintala, and Gregory Chanan. Pytorch, 2017. 5, 6
- [30] Ao Ren, Tianyun Zhang, Shaokai Ye, Wenyao Xu, Xuehai Qian, Xue Lin, and Yanzhi Wang. Admm-nn: an algorithm-hardware co-design framework of dnns using alternating direction methods of multipliers. In *ASPLOS*, 2019. 8
- [31] Karen Simonyan and Andrew Zisserman. Very deep convolutional networks for large-scale image recognition. *arXiv preprint arXiv:1409.1556*, 2014. 6

- [32] Ma Siyuan, Bassily Raef, and Belkin Mikhail. The power of interpolation: Understanding the effectiveness of sgd in modern over-parametrized learning. In *2018 International Conference on Machine Learning (ICML)*. ACM/IEEE, 2018. [3](#)
- [33] Jost Tobias Springenberg and Thomas Brox and Martin Riedmiller Alexey Dosovitskiy. Striving for simplicity: The all convolutional net. In *ICLR-2015 workshop track*, 2015. [7](#)
- [34] Wei Wen, Chunpeng Wu, Yandan Wang, Yiran Chen, and Hai Li. Learning structured sparsity in deep neural networks. In *Advances in neural information processing systems*, pages 2074–2082, 2016. [1](#), [2](#)
- [35] Mengwei Xu, Mengze Zhu, Yunxin Liu, Felix Xiaozhu Lin, and Xuanzhe Liu. Deepcache: Principled cache for mobile deep vision. In *Proceedings of the 24th Annual International Conference on Mobile Computing and Networking*, pages 129–144. ACM, 2018. [2](#)
- [36] Shuochao Yao, Shaohan Hu, Yiran Zhao, Aston Zhang, and Tarek Abdelzaher. Deepsense: A unified deep learning framework for time-series mobile sensing data processing. In *Proceedings of the 26th International Conference on World Wide Web*, 2017. [2](#)
- [37] Jiahui Yu and Thomas Huang. Autoslim: Towards one-shot architecture search for channel numbers. *arXiv preprint arXiv:1903.11728*, 2019. [8](#)
- [38] Chenglong Zhao, Bingbing Ni, Jian Zhang, Qiwei Zhao, Wenjun Zhang, and Qi Tian. Variational convolutional neural network pruning. In *Proceedings of the IEEE Conference on Computer Vision and Pattern Recognition*, pages 2780–2789, 2019. [8](#)
- [39] Zhuangwei Zhuang, Mingkui Tan, Bohan Zhuang, Jing Liu, Yong Guo, Qingyao Wu, Junzhou Huang, and Jinhui Zhu. Discrimination-aware channel pruning for deep neural networks. In *Advances in Neural Information Processing Systems*, pages 875–886, 2018. [8](#)